

Article

Statistical Determination of a Fretting-Induced Failure of an Electro-Deposited Coating

Kyungmok Kim

School of Aerospace and Mechanical Engineering, Korea Aerospace University, 76 Hangeongdaehang-ro, Deogyang-gu, Goyang-si, Gyeonggi-do 412-791, Korea; kkim@kau.ac.kr; Tel.: +82-2-300-0288

Academic Editors: Eva Pellicer and Jordi Sort

Received: 22 February 2017; Accepted: 29 March 2017; Published: 31 March 2017

Abstract: This paper describes statistical determination of fretting-induced failure of an electro-deposited coating. A fretting test is conducted using a ball-on-flat plate configuration. During a test, a frictional force is measured, along with the relative displacement between an AISI52100 ball and a coated flat specimen. Measured data are analyzed with statistical process control tools; a frictional force versus number of fretting cycles is plotted on a control chart. On the control chart, critical number of cycles to coating failure is statistically determined. Fretted surfaces are observed after interrupting a series of fretting tests. Worn surface images and wear profiles provide that the increase on the kinetic friction coefficient after a steady-state sliding is attributed to the substrate enlarged at a contact surface. There is a good agreement between observation of worn surfaces and statistical determination for fretting-induced coating failure.

Keywords: electro-deposited coating; coating failure; fretting; statistical process control

1. Introduction

In the design of tribo-components, it is essential to evaluate the tribological properties of the components, since they crucially affect the performance of an entire system. In order to minimize friction between two mating components, solid coatings are often applied into contact surfaces. Evaluation of a solid coating is carried out with a simplified tribotest, prior to a field test [1]. In a tribotest, a coating is evaluated with the kinetic friction coefficient or the wear rate under the conditions similar to those found in actual contact situations. The wear rate of a coating was typically calculated by measuring volumetric loss of materials after a series of wear tests [2,3]. The kinetic friction coefficient is a useful indicator because it is possible to measure the coefficient in the course of a friction test. Some studies evaluated tribological performances of solid coatings on the basis of a kinetic friction coefficient evolution [4–6]. Fretting tests with thermally sprayed solid coatings were terminated when the kinetic friction coefficient reached the critical value similar to those observed at the substrate-to-substrate contact. Then, the number of cycles to the critical value was taken into account as the fretting lifetime of a solid coating [5,6]. Meanwhile, the endurance life of a coating was proposed as the number of fretting cycles when the friction coefficient came to be three times greater than the initial value [4]. The dissipated energy approach was used to establish the durability and the safe running time of a coating under fretting conditions [7]; an energy-Wohler wear chart was introduced, in which the critical dissipated energy density corresponded to the time when a coating wore off.

Electro-deposited coatings are widely used for automotive components because they maintain high corrosion resistance. Electro-deposited coatings are often applied to frictional contacts such as automotive seat sliding rails. In the previous studies with epoxy-based electro-deposited coatings, there were difficulties in determining the durability of the coating with the criteria described above; the coating was found to fail earlier than the critical values proposed by the criteria [8]. Thus, an adequate method is needed for determining the fretting lifetime of electro-deposited coatings.

Statistical process control (SPC) is a well-established technique for ensuring process quality, thereby being used in manufacturing and production industries. Particularly, SPC tools were successfully used for monitoring a manufacturing process subjected to tool wear [9,10]. For monitoring tool wear, SPC tools allowed distinguishing two sources of variation; one was natural variability, and the other was special causes such as improperly adjusted tools, operator errors, and inferior raw materials. In SPC, measured output data (e.g., surface roughness) were analyzed with control charts such as the average \bar{x} -bar chart and a range chart. Measured data from a process without special causes were placed between the upper and the lower control limits on the average \bar{x} -bar chart. If some data were found beside the control limits, a process was considered to be instable, said to be out of control. Thus, it was possible to detect a process that became out of control.

For monitoring the state of a cutting tool, acoustic emission signals were measured and analyzed with SPC tools [11]. SPC tools were used for predicting the formation of voids and defects in friction stir welding [12]. Variance of process forces was found to be correlated to the formation of defects in friction stir welds. SPC was used for detecting faults in a bearing [13–15]. Parameters indicating the state of a bearing were measured and analyzed with SPC tools. The parameters included vibration, stator current noise, and bearing housing temperature. A set of vibration data measured in a rolling element ball bearing was evaluated with SPC control tools [13]. Instead of vibration, stator current noise was monitored for detecting in situ bearing faults [14]. Housing temperature of a sliding bearing was determined in dry friction conditions [15]. Change of housing temperature in the course of a test was used for identifying the state of bearing condition. However, it is necessary to exclude the variance of housing temperature that arises from the change of room temperature.

In this study, a fretting test was conducted with an electro-deposited coating used for automotive seat tracks. In order to develop a criterion to identify the failure of a fretted electro-deposited coating, statistical analysis was employed with measured frictional force data. Control charts in statistical process control technique were used to identify the transition of the frictional force. Additionally, fretted surfaces were captured and wear profiles were measured to observe surface damages at various numbers of fretting cycles. Finally, comparison between observation of the wear profile and statistical determination was employed.

2. Materials and Methods

Figure 1 shows an in-house developed fretting machine used for this study. The fretting machine enables the linear reciprocating motion of a flat specimen to a fixed counterpart. The reciprocating motion was imposed in a sine wave. The relative displacement between a specimen and a counterpart (ball) was continuously measured with a laser displacement sensor (Model LK-081, a resolution of 0.003 mm and a linearity of $\pm 0.1\%$, Keyence Corp., Itasca, IL, USA). A cylindrical ball holder was permitted to vertical movement in a rigid arm. Dead weights were placed on the holder for the purpose of inducing normal force at the contact between a flat specimen and a ball. A load-cell (Interface, Inc., Atlanta, GA, USA) was connected to a rigid arm for measuring frictional force. In this study, a commercial AISI 52100 steel ball (a diameter of 5 mm and R_a of about 0.025 μm) was used as a counterpart.

In this study, a normal force of 49 N, a displacement amplitude of 0.2 mm, and a frequency of 1 Hz were applied to produce fretting damage on a flat specimen. The magnitude of normal force was similar to those found in the automotive seat slide tracks.

An epoxy-based cathodic electro-deposited coating was applied onto the substrate of a flat specimen (high-strength steel, material designation: SPFC 440); in order for the coating layer to be deposited on the substrate, the substrate was immersed in a tank filled with the electrocoat and connected to a rectifier as the corresponding electrode. The counter electrode was immersed at the same time and a direct charge was provided under the conditions described in Table 1. The coating contained an epoxy resin with a metal catalyst and a crosslinker of blocked aromatic isocyanates. Figure 2 shows the microstructure image of an electro-deposited coating. The thickness of a deposited coating was

dependent upon parameters such as applied voltage, electro-deposited (ED) time, and pH. In this study, the coating thickness on the substrate was measured with a microscope; the initial coating thickness was $22 \pm 2 \mu\text{m}$ and the arithmetic average roughness (R_a) of the coating was $0.518 \pm 0.051 \mu\text{m}$. Pencil hardness of the coating was 5H (corresponding to about 34.9 in Knoop hardness). Fretting tests were conducted with the specimen having a coating thickness of $22 \mu\text{m}$ for minimizing the effect of coating thickness on a frictional force evolution. All tests were conducted under room temperature (about 25°C) and ambient humidity (about 55% RH).

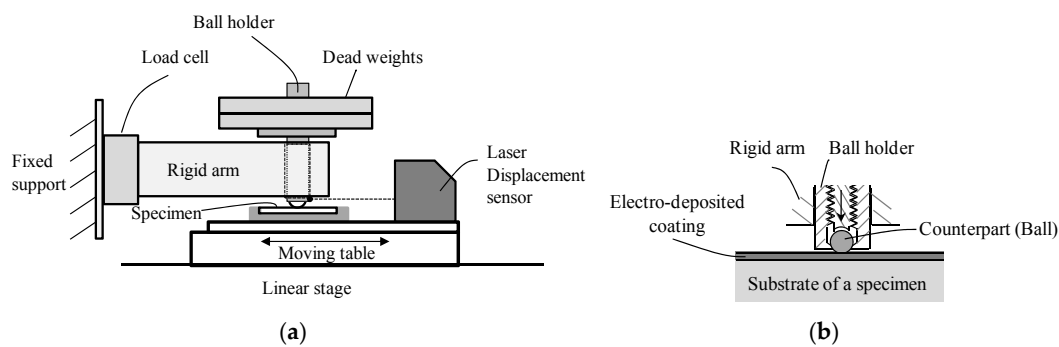


Figure 1. A schematic diagram of a fretting testing machine: (a) test rig; (b) ball-on-flat plate contact.

Table 1. Condition of cathodic electro-deposition.

Specification	Value
Solid content	15%–22%
Pigment binder ratio	0.15
pH	5.9–6.3
Conductivity	120–180 $\mu\text{S}/\text{mm}$
Voltage	230–290 V
Electro-deposition (ED) time	About 180 s

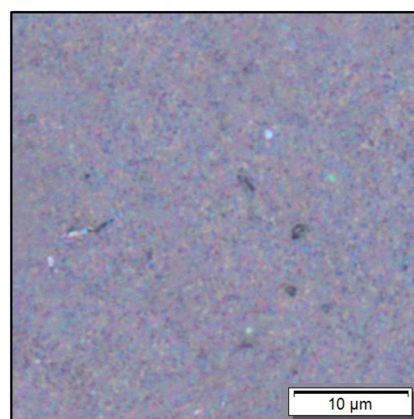


Figure 2. Microstructure image of an electro-deposited coating.

3. Results and Discussion

A fretting test was conducted at the displacement amplitude of 0.2 mm, a normal force of 49 N, and a frequency of 1 Hz. The test was terminated at the friction of 25 N; it was identified from the previous studies that the kinetic friction between an AISI 52100 steel ball and a high strength steel plate was about 25 N at a normal force of 49 N [8]. During a test, a frictional force and the relative displacement between a ball and a plate were recorded.

Figure 3 shows a fretting loop with respect to number of cycles. All fretting loops were quasi-rectangular shaped. Frictional force peaks were observed in the loops found at the 750th and 800th cycles due to ploughing effect. Figure 4 shows the evolution of a slip ratio for an electro-deposited coating at the displacement amplitude of 0.2 mm. A slip ratio was defined as the ratio of an actual sliding distance to a total displacement. The actual sliding distance was determined when a frictional force was zero on a fretting loop. It was identified that the transition between a reciprocal sliding regime and a fretting regime (gross slip) was observed at a slip ratio of 0.95 [16]. As shown in Figure 4, all slip ratios remained lower than 0.95, ensuring that a test was completed within a gross slip regime.

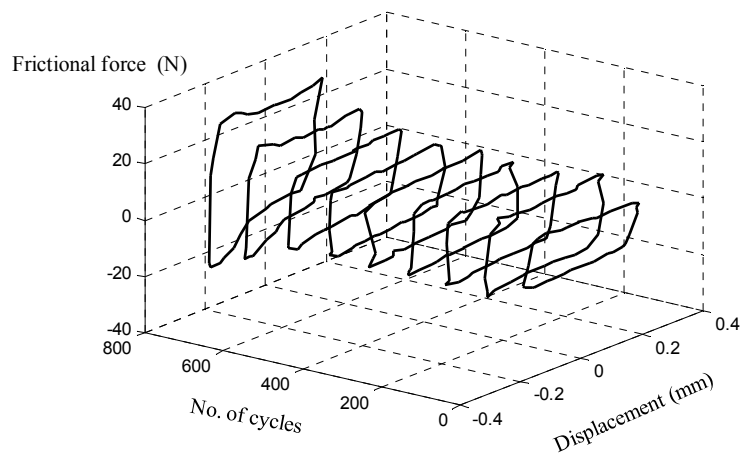


Figure 3. Fretting loops of an electro-deposited coating at a normal force of 49 N, an imposed displacement amplitude of 0.2 mm, and a frequency of 1 Hz.

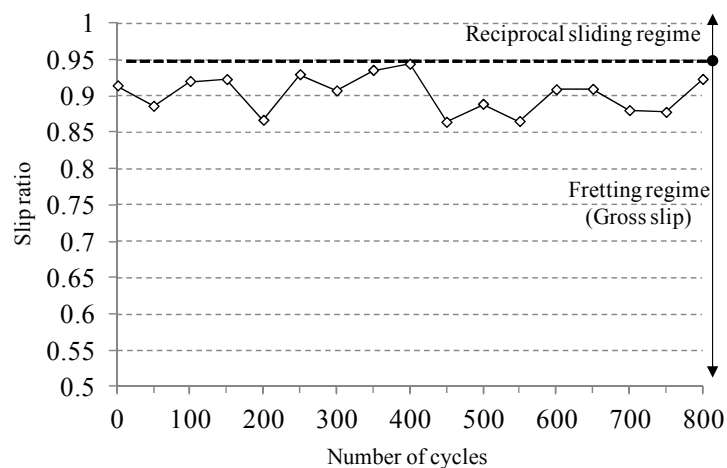


Figure 4. Slip ratios of an electro-deposited coating at a normal force of 49 N, an imposed displacement amplitude of 0.2 mm, and a frequency of 1 Hz.

For statistical analysis, two frictional forces were selected on a fretting loop: The maximum value and the force at zero displacement (movement to the left side). Note that the forces could be identified apparently in a fretting loop and the maximum value is used for determine the coefficient of kinetic friction. The two force values were then averaged. Figure 5 shows the average frictional force with respect to number of cycles. The initial value was 8.63 N. After the initial increase, the value remained almost steady (so-called steady-state sliding stage). During steady-state sliding, variance of the frictional force was attributed to surface roughening of an electro-deposited coating layer. In addition, wear debris formed might remain within the contact zone. After 600 cycles, the average frictional force was determined to increase rapidly; wear debris might be removed from the contact zone.

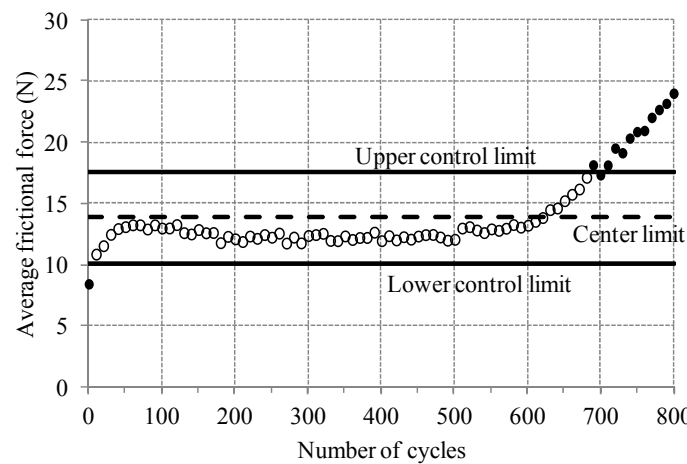


Figure 5. Evolution of the average frictional force and control limits.

Analysis of statistical process control (SPC) was employed with the average frictional forces. The purpose of the statistical analysis was to distinguish two sources of variation; one was surface roughening of a coating layer, and the other was the partial contact between the ball and the substrate. In order to determine the cycle when the partial contact occurs between the ball and the substrate, the following procedure was employed:

- The average frictional force versus the number of cycles plot was obtained. In addition, the difference between two selected frictional values was plotted over the number of cycles. The difference was called Range (*R*).
- Control limits for the average and the range were calculated according to Tables 2 and 3.
- Control limits were then plotted on the average frictional force evolution (the average *x*-bar chart) and *R*-chart as shown in Figures 5 and 6.
- After excluding the data that were out of control limits, control limits were revised.
- When all data remained between the revised control limits, the revision was terminated, and the final cycle was proposed as the one that the partial contact started to occur between the ball and the substrate.

Table 2. Definitions of control limits for the average frictional force chart. \bar{Q} and N_s denote the average frictional force and the number of subgroups, respectively. A_2 is 1.88 for two sample sizes. *R* is the difference between selected frictional forces.

Control Limit	Definition
Center limit (CL)	$\frac{\sum \bar{Q}}{N_s}$
The upper control limit (UCL)	$CL + A_2 \times \frac{\sum R}{N_s}$
The lower control limit (LCL)	$CL - A_2 \times \frac{\sum R}{N_s}$

Table 3. Definitions for *R*-chart. *R* is the range between selected frictional forces. N_s denotes number of subgroups. D_3 and D_4 denote the constants, and they were zero and 3.267, respectively.

Control Limit	Definition
Center limit (CL _R), \bar{R}	$\frac{\sum R}{N_s}$
The upper control limit (UCL _R)	$D_4 \times \bar{R}$
The lower control limit (LCL _R)	$D_3 \times \bar{R}$

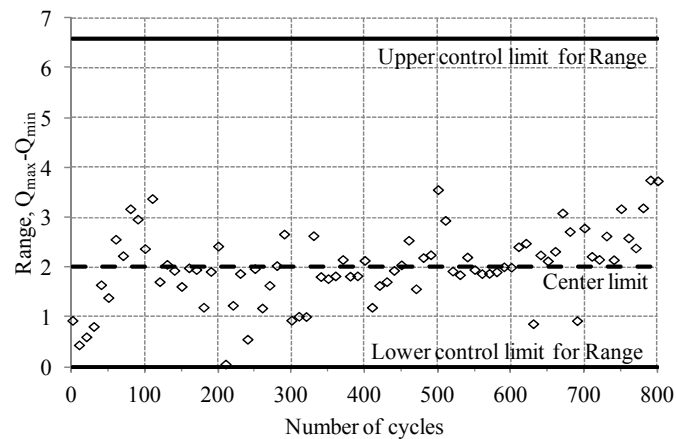


Figure 6. R-chart for the difference between selected frictional forces.

Figure 5 shows the evolution of the average frictional force (\bar{Q}) with three control limits. Control limits for the average frictional force evolution were determined with the parameters shown in Table 2. \bar{Q} and N_s denote the average frictional force and the number of subgroups, respectively. In this study, a subgroup is associated with a cycle. Each subgroup contained two frictional force values. The constant, A_2 , is dependent upon the sample size ($A_2 = 1.88$ for two samples in one subgroup [17]). R is the difference between selected frictional forces. In this study, the total number of cycles was 800, and the cycle interval was 10. Thus, the number of subgroups was 80. If all of the average frictional forces were placed between the upper control limit and the lower control limit in the chart, a process was considered as in control. That is, the “in-control process” can be defined as the state that a ball slid on a coating layer. Small variance of the frictional force was attributed to the surface roughening of a coating layer. If the average value exceeded the upper control limit, a process became statistically out of control. It means that a ball partially slid on the surface of the substrate. That is, an out-of-control process might correspond to the state that some parts of a coating layer wore off. In Figure 5, dark solid markers were placed outside the control limits; the first value remained below the lower control limit, while other values after 670 cycles were above the upper control limit. The first value was the average frictional forces measured during the initial running-in period. Thus, one could exclude the initial value in determining coating failure.

Figure 6 shows Range (R) chart for a fretted electro-deposited coating. The Range was defined as the difference between selected frictional forces found in a fretting loop. The upper and the lower control limits, and the center limit for R-chart were defined as Table 3. The constants, D_3 and D_4 , are dependent upon selected sample size ($D_3 = 0$ and $D_4 = 3.267$ for two samples in each subgroup [17]). It was identified from Figure 6 that all range values were found to remain between the upper and the lower control limits.

For the purpose of additional analysis, the average frictional forces outside the upper and the lower control limits in Figure 5 were removed and then statistical analysis was re-employed; control limits were recalculated. On the modified frictional force chart, some data exceeded the upper control limit. Thus, the control limits were revised after excluding the data that exceeded the control limit. Figure 7 shows the revised chart for the average frictional force. It was identified from the plot that all values were placed between two control limits, indicating that a ball slid on a coating layer by the 670th cycle. In other words, it could be suggested that the durability of an electro-deposited coating was 670 fretting cycles at a given test condition.

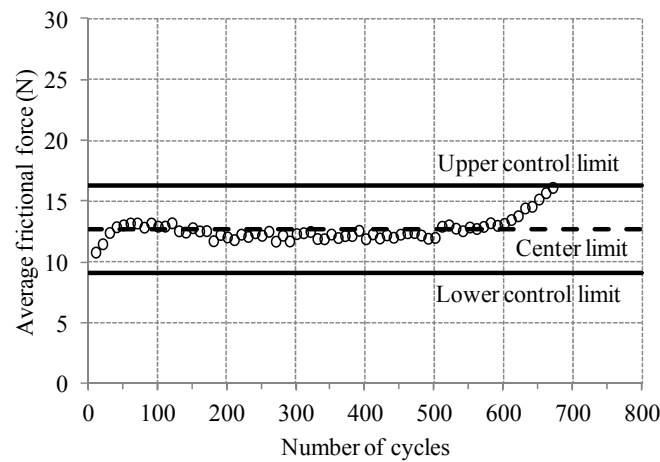


Figure 7. The revised average \bar{x} -bar chart for the evolution of the average frictional force. Control limits were revised.

In order to observe surface damages under the fretting condition, fretting tests were interrupted at various numbers of cycles. The coefficient of the kinetic friction was determined during a fretting test. The kinetic friction coefficient was defined as the ratio of the maximum frictional force to the imposed normal force. Fretted surface images were captured by optical microscope ($250\times$) (Shenzhen Supereyes Technology Co., Ltd., Shenzhen, Guangdong, China) and wear profiles were measured by surface profilometer (Mitutoyo Corp., Takatsuku, Kawasaki, Japan). Figure 8 shows the fretting images at various numbers of cycles. After the initial cycle, a crater was observed. At the 100th cycle, the crater became bigger. At the 500th cycle, a coating layer was observed to remain within the contact zone. Wear profile shows that the substrate did not appear in the contact. Note that the average coating thickness was 0.022 mm. Bright areas near contact edges were due to the reflection of light during image capture. Measured wear profile at the 700th cycle shows that the maximum wear depth exceeded the coating depth, indicating that the substrate appeared at the contact. It can be identified that the increase on the friction coefficient was attributed to the ball-on-substrate contact. At the 800th cycle, it was observed that the entire contact surface was severely damaged and the substrate was roughened along the direction parallel to the sliding direction.

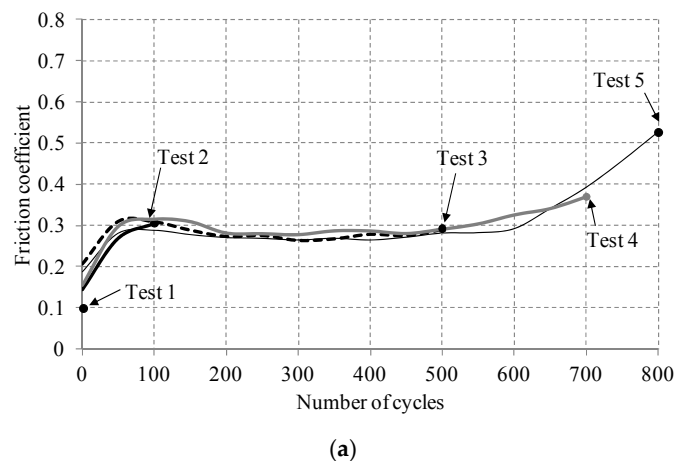


Figure 8. Cont.

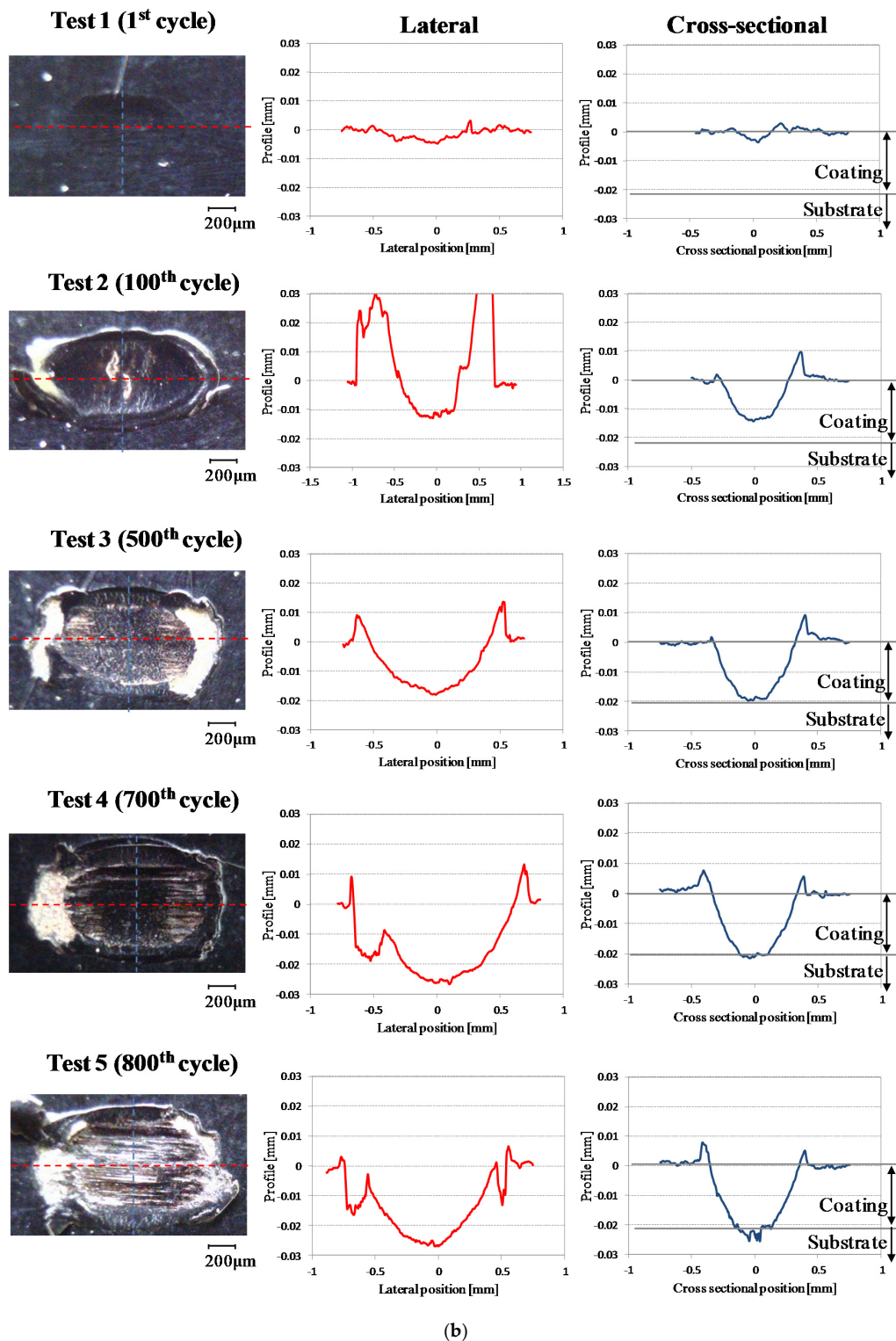


Figure 8. Measurement of the friction coefficient and observation of fretted surfaces: (a) the friction coefficient evolution; (b) worn surface images (250×) and surface profiles. Note that the initial coating thickness was 0.022 mm. Bright areas near contact edges were associated with reflection of light in a microscope.

Figure 9 shows the ratio of the maximum wear depth to initial coating thickness. The maximum wear depth ratio of greater than unity indicates that some parts of the coating in a contact zone wore off

and the ball slid on the surface of the substrate. It was shown that the maximum wear depth exceeded the initial coating depth between the 500th and the 700th cycles. This is in good agreement with statistical analysis result; in the statistical analysis, the critical cycle for in-control process was the 670th cycle. Therefore, one might consider the 670th cycle as the durability of a fretted electro-deposited coating under the given test conditions.

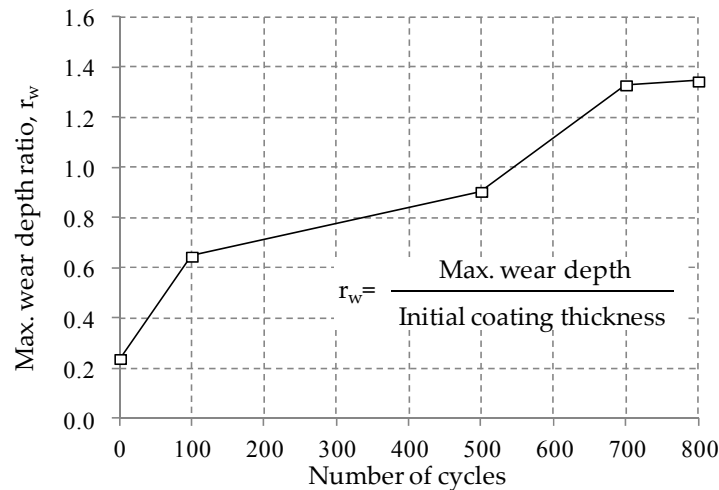


Figure 9. The maximum wear depth evolution according to number of cycles. The maximum wear depth ratio defined as the ratio of the maximum wear depth to initial coating thickness.

In this study, fretting was induced to the contact between an electro-deposited coating and an AISI 52100 steel ball. Thus, the displacement amplitude of greater than 0.2 mm needs to be taken into account for determining the failure of an electro-deposited coating under a reciprocal sliding condition. In addition, other solid lubricant coatings need to be evaluated with the proposed statistical method. In this statistical analysis, two frictional forces in a fretting loop were selected. Thus, future work needs to include additional force selection in a fretting loop for statistical analysis.

4. Conclusions

This paper investigated the fretting-induced failure of a cathodic electro-deposited coating for automotive components. A frictional force and the relative displacement between a specimen and a counterpart were measured during a fretting test. Statistical analysis was employed with measured frictional forces. The following conclusions were drawn:

- Control charts in statistical process control were found to be useful for identifying the quality of a fretted electro-deposited coating in terms of the kinetic friction coefficient. It was identified that control charts could detect the cycle when the kinetic friction became instable.
- Optical observation of worn surfaces and measurement of wear profiles showed that the coating was found to fail partially at the cycle when the kinetic friction coefficient increased.
- It could be suggested that the durability of the fretted electro-deposited coating can be defined as the cycle when the average value of frictional forces exceeded the upper control limit on the charts.

Future work needs to include reciprocal sliding tests with various solid lubricant coatings, and various counterparts such as stainless steel and ceramic balls. Additional force selection per cycle would be useful for accurate statistical analysis.

Acknowledgments: This work was supported by the National Research Foundation of Korea (NRF) grant funded by the Korean government (MSIP) (No. 2016R1C1B1008483).

Conflicts of Interest: The authors declare no conflict of interest.

References

1. Bhushan, B. *Introduction to Tribology*, 1st ed.; John Wiley & Sons, Inc: New York, NY, USA, 2002.
2. Fouvry, S.; Kapsa, P.; Vincent, L. Analysis of sliding behaviour for fretting loadings: Determination of transition criteria. *Wear* **1995**, *185*, 35–46. [[CrossRef](#)]
3. Nallasamy, P.; Saravanakumar, N.; Nagendran, S.; Suriya, E.M.; Yashwant, D. Tribological investigations on MoS₂-based nanolubricant for machine tool slideways. *Proc. Inst. Mech. Eng. Part J J. Eng. Tribol.* **2015**, *229*, 559–567. [[CrossRef](#)]
4. Langlade, C.; Vannes, B.; Taillandier, M.; Pierantoni, M. Fretting behavior of low-friction coatings: Contribution to industrial selection. *Tribol. Int.* **2001**, *34*, 49–56. [[CrossRef](#)]
5. Korsunsky, A.M.; Torosyan, A.T.; Kim, K. Development and characterization of low friction coatings for protection against fretting wear in aerospace components. *Thin Solid Films* **2008**, *516*, 5690–5699. [[CrossRef](#)]
6. Kim, K.; Korsunsky, A.M. Dissipated energy and fretting damage in CoCrAlY-MoS₂ coatings. *Tribol. Int.* **2010**, *43*, 676–684. [[CrossRef](#)]
7. Liskiewicz, T.; Fouvry, S.; Wendler, B. Development of a Wöhler-like approach to quantify the Ti(C_xN_y) coatings durability under oscillating sliding conditions. *Wear* **2005**, *259*, 835–841. [[CrossRef](#)]
8. Kim, K. A study of the frictional characteristics of metal and ceramic counterfaces against electro-deposited coatings for use on automotive seat rails. *Wear* **2014**, *320*, 62–67. [[CrossRef](#)]
9. Wu, Z. An adaptive acceptance control chart for tool wear. *Int. J. Prod. Res.* **1998**, *36*, 1571–1586. [[CrossRef](#)]
10. Motorcu, A.R.; Gullu, A. Statistical process control in machining, a case study for machine tool capability and process capability. *Mater. Des.* **2006**, *27*, 364–372. [[CrossRef](#)]
11. Houshmand, A.A.; Kanatey-Ahibu, E. Statistical process control of acoustic emission for cutting tool monitoring. *Mech. Syst. Signal. Process.* **1989**, *3*, 405–424. [[CrossRef](#)]
12. Jata, K.V.; Mahoney, M.W.; Mishra, R.S. *Friction Stir Welding and Processing III*, 1st ed.; Wiley: Hoboken, NJ, USA, 2005.
13. Wang, W.; Zhang, W. Early defect identification: application of statistical process control methods. *J. Qual. Mainten. Eng.* **2008**, *14*, 225–236. [[CrossRef](#)]
14. Zhou, W. Bearing fault detection via stator current noise cancellation and statistical control. *IEEE. Trans. Ind. Electron.* **2008**, *55*, 4260–4269. [[CrossRef](#)]
15. Lepiarczyk, D.; Gawedzki, W.; Tarnowski, J. Thermal analysis of the friction process of sliding bearings using a statistical approach. *Tribologia* **2016**, *4*, 157–165.
16. Varenberg, M.; Etsion, I.; Halperin, G. Slip index: A new unified approach to fretting. *Tribol. Lett.* **2004**, *17*, 569–573. [[CrossRef](#)]
17. Montgomery, D.C. *Introduction to Statistical Quality Control*, 6th ed.; John Wiley & Sons, Inc.: New York, NY, USA, 1997.

